IEEE Access
Multidisciplinary | Rapid Review | Open Access Journal

Received June 23, 2020, accepted July 20, 2020, date of publication July 23, 2020, date of current version August 14, 2020.

Digital Object Identifier 10.1109/ACCESS.2020.3011625

Multi-Parameter Optimization Method for Remaining Useful Life Prediction of Lithium-Ion Batteries

BING LONG, (Member, IEEE), XIAOYU GAO, PENGCHENG LI, AND ZHEN LIU
School of Automation Engineering, University of Electronic Science and Technology of China (UESTC), Chengdu 611731, China

Corresponding author: Bing Long (longbing@uestc.edu.cn)

This work was supported in part by the National Natural Science Foundation of China under Grant U1830133.

ABSTRACT Accurate prediction of the remaining useful life (RUL) of lithium-ion batteries can ensure the normal and effective operation of power systems using lithium-ion batteries. However, how to select battery prediction parameters through scientific methods and how to accurately predict battery RUL values under high and low temperature conditions are still a huge challenge. Thus according to the technique for order preference by similarity to ideal solution (TOPSIS) based on information entropy, improved particle swarm optimization (PSO) and moving average filter(MAF), a novel data-driven method for predict lithium-ion batteries' RUL is proposed. The TOPSIS method based on information entropy is proposed to select the best degradation parameters; a sliding average low-pass filter is used to solve the capacity regeneration and noise problem of the battery experimental data; the improved PSO algorithm is presented to predict the battery RUL accurately. Based on the batteries experimental data from NASA and University of Maryland, we have done many simulation experiments on parameters selection and RUL accuracy comparisons among several data-driven methods. The experimental results shows:(1) compared with the other prediction methods without degradation parameters selection, the proposed method with TOPSIS and MAF filtering is more accurate;(2) our proposed algorithm has higher prediction accuracy and use less training data than other data-driven algorithms;(3) this method has high prediction accuracy under both the high and low temperature conditions.

INDEX TERMS Lithium-ion batteries, remaining useful life (RUL), technique for order Preference by similarity to ideal solution(TOPSIS) method, improved particle swarm optimization(PSO), moving average filter(MAF).

I. INTRODUCTION

Compared with the traditional lead-acid batteries, nickel-cadmium batteries and nickel-hydrogen batteries, lithium-ion batteries have many advantages, such as high relative energy density, light weight, long life and fast charge-discharge. Therefore, lithium-ion batteries are now widely used in civil electronic products, such as mobile phones, computers and Bluetooth headsets; they are also widely used in low emission energy saving electric vehicles and in large-scale production such as aerospace systems, military communications [1]–[3]. Therefore, the failures caused by the decay of the life of the lithium-ion battery may cause degradation or damage to the device. The light failures make the machines unusable, and the fatal failures endanger the personal safety. For example, the improper management of lithium-ion batteries in electric vehicles caused the fire and explosion [4]. In the field of aerospace, the power system failure caused by lithium-ion battery is the main cause of system failure [1], [5].

Therefore, in order to ensure the normal operation of the large systems with lithium-ion batteries, the most important issue is to predict the battery remaining useful life (RUL) accurately.

In order to predict the RUL of a lithium-ion battery accurately, it is necessary to monitor the battery status. In general, the state-of-health (SOH) is used to describe the battery health status [6]. SOH is generally expressed as a decrease in effective capacity or an increase in internal resistance [7], [8]. EOL indicates the end-of-life time of lithium-ion batteries. When SOH reaches EOL, the battery can no longer be

The associate editor coordinating the review of this manuscript and approving it for publication was Jenny Mahoney.

available [6], [9]–[11]. In general, when the SOH drops to 80% of the rated capacity, it means the battery reaches EOL and must be replaced [12].

The RUL prediction methods of lithium-ion batteries can be divided into model-based prediction methods and data-driven prediction methods [1]. Model-based methods can perform detailed physical and chemical analysis of the battery aging process [13]–[16]. But the models are based on specific environmental conditions and charging, discharging conditions. The parameters in the models are obtained according to the physical characteristics and environmental variables of the batteries. So the model parameters are complex and difficult to change with the battery working conditions. Due to its high complexity, it is impossible to predict the RUL efficiently and accurately.

The data-driven prediction methods don't consider the aging mechanism inside the lithium-ion battery, and the battery RUL can directly achieved based on the battery performance test data and status monitoring data. Wei *et al.* [2] proposed a method to predict RUL of lithium-ion batteries by means of particle filtering (PF) and support vector regression (SVR). The internal resistance and cycle number of the battery were selected as parameters of the degradation model and a good RUL prediction result was achieved. The Wei's method has a large amount of training calculation and is prone to over-fitting. So there are some problems in efficiency. Jin *et al.* [3] predicted the RUL of lithium-ion batteries through an improved odorless particle filtering method, and the battery cycle number were used as the model's degradation parameter. The results show that the improved particle filtering method has some improvements compared with the traditional particle filtering methods. But its parameters selection is subjective and unscientific. Based on the local information fusion and support vector regression, Chaoui *et al.* [8] proposed an integration algorithm to predict RUL of lithium-ion batteries. The local information fusion of data is used to replace the original global information, so the information layer fusion problem is transformed into a decision layer fusion problem [8]. Erdinc *et al.* [15] constructed a high-fidelity battery model through multi-objective constrained nonlinear optimization technology and derived a charging mode suitable for lithium-ion batteries. Wang *et al.* [17] proposed a method for lithium-ion batteries RUL based on the Verhulst model, particle swarm optimization and particle filtering. Xian *et al.* [18] predicted RUL of lithium-ion batteries based on spherical volume particle filter. Liu *et al.* [13] proposed a ARD-based GPR model for model training, verification and comparison of battery calendar aging experimental data, and obtained more accurate prediction results. On this basis, they compared the performance of the solo-GPR, solo-LSTM, GPR+EMD and LSTM+EMD models, and found that the prediction effect of the LSTM+GPR combined model is better than other models [14].

The data-driven RUL predicted mentioned above are too subjective in the parameter selection of the prediction model and had little scientific basis. Only the number of cycles was selected as the model parameter in [3], [10], [18], [19]. In this case, the degradation mechanism and environmental factors of the battery are not considered. The selected parameters in reference [2] do not change with the working conditions. Different parameters data have different states under different working conditions. Some of them are suitable for battery RUL prediction while others are not. Therefore, we should use a scientific method to select best parameters of battery degradation model. In terms of raw data processing, the above methods did not eliminate the noise of the original data through filtering. Moreover, the noise of the original data affected the efficiency of model and made the model parameters fluctuate, which leaded to the inaccurate prediction result. Finally, none of the above literature has predicted the battery life under both the high or low temperature conditions accurately. To solve the three problems, according to the technique for order preference by similarity to ideal solution (TOPSIS) based on information entropy, improved particle swarm optimization (PSO) and moving average filter(MAF), a novel data-driven method for predict lithium-ion batteries' RUL is proposed in this paper.

The work of this paper is organized as follows. Section II discusses the degradation mechanism of lithium-ion batteries and selects suitable degradation parameters for prediction model. Section III presents the methods of parameter optimization, data filtering and model training under different working conditions. Section IV establishes the overall experimental framework. Section V gives the experimental results and compares them. Section VI concludes all the work.

II. SELECTION OF DEGRADATION PARAMETRRS FOR LITHIUMION BATTERIRS

In order to select the appropriate degradation parameters to predict the RUL of lithium-ion batteries, it is necessary to understand the capacity degradation mechanism of lithium-ion batteries. Lithium-ion batteries usually use graphite as anode material, lithium compounds ($LiCoO_2$) as cathode, $LiPf_6$ and alkyl carbonates (such as vinyl carbonate (EC) and diethyl carbonate (DEC) as electrolytes [20]. During the charge-discharge cycle of lithium-ion batteries, the redox reaction consumes active materials, and excess products are deposited on the negative electrode [21]. The main causes of capacity loss of lithium-ion batteries are as follows: (1) growth of solid electrolyte membranes (SEI) [22]; (2) increase of internal resistance of batteries [23]; (3) consumption of active substances [24]–[26].

The amount of chemical reaction products generally increases with the change of reaction time, while the amount of reactants decreases with the change of reaction time. Therefore, the thickness of SEI film and the loss of active substances will change with the increase of the service time of lithium-ion batteries, i.e. the number of charge-discharge cycles N. In many references [17]–[19], the number of charge-discharge cycles of lithium-ion batteries is used as the first prediction parameter for estimating RUL of batteries.

However, during the operation of a lithium-ion battery, load conditions and operating conditions may change sometimes. For example, changes in temperature T can cause changes in the rate of chemical reactions. In addition, the internal resistance of batteries and the impedance response of SEI films are also related to temperature [22]. The output voltage of the lithium-ion battery under different charging and discharging conditions, temperature and cycling conditions was simulated, and a dynamic degradation model of the lithium-ion battery was established [16]. An electric and thermal model of a hybrid electric vehicle (HEV) lithium-ion battery pack at low temperature was established [27]. Mejdoubi A E *et al.* predicted SOC and SOH of batteries at different operating temperatures by extended Kalman filter (EKF) [7]. Therefore, the working temperature of lithium-ion battery is taken as the second model parameter for RUL prediction.

The internal resistance of lithium-ion batteries is composed of electrolyte resistance Re and charge transfer resistance Rct. Normally, the battery's internal resistance R of the battery is the sum of the two. The capacity and power loss of lithium-ion batteries will increase the internal resistance of lithium-ion batteries [28], [29]. Yuan H F *et al.* estimated RUL of batteries by estimating charge transfer resistance [30]. Schmidt A P *et al.* use the resistance R and the battery capacity to predict the RUL value of the battery [31]. According to the above references and observation of battery data, the internal resistance of lithium-ion batteries is closely related to the capacity degradation of lithium-ion batteries, so we consider the internal resistance of lithium-ion batteries as the third degradation parameter of RUL estimation of lithium-ion batteries.

The open-circuit voltage of a battery is the value of the battery voltage which reaches a steady state after a cycle of full charge and discharge. We mark it as Vdischarge. In this paper, the open-circuit voltage of a battery is represented by the battery voltage one minute after the battery is open-circuit. By analyzing the relationship between the remaining capacity data of the battery and its open-circuit voltage, there is a great correlation between them, therefore the open-circuit voltage of lithium-ion batteries is chosen as the forth degradation parameter of lithium-ion batteries.

III. RELATED METHOD

A. TOPSIS METHOD

The TOPSIS method was originally proposed by Hwang and Yoon to rank the schemes by evaluating the indicators of multiple schemes [32]. TOPSIS method finds the best scheme by obtaining the distance from each scheme to the ideal solution and the distance from each scheme to the negative ideal solution [33]. The TOPSIS method for parameter optimization is used in this paper. The basic steps of TOPSIS are as follows:

Step 1) Forming the decision matrix:

Let the set of schemes for multi-index decision-making be $M = (M1,M2,M3\ldots Mm)$ The evaluation indicators of each scheme are as follows: $C = (C1,C2,C3\ldots Cn)$ The value of scheme Mj to index Ci is recorded as X_{ij} $(j = 1,2,\ldots m;$ $i = 1,2,\ldots n)$. The multi-objective decision matrix X is as follows

$$x = \begin{pmatrix} x_{11} & \cdots & x_{1n} \\ \vdots & \ddots & \vdots \\ x_{m1} & \cdots & x_{mn} \end{pmatrix} \tag{1}$$

Step 2) Standardizing the decision matrix

In order to eliminate the influence of each index dimension on scheme decision-making, it is necessary to perform a dimensionless process on the decision matrix and construct standardized decision matrix $V = (v_{ij})_{m\times n}$.

The better dimensionless process for the big indexes is:

$$v_{ij} = \left(x_{ij} - \min_j x_j\right) / \left(\max_j x_j - \min_j x_j\right) \tag{2}$$

The better dimensionless process for the small indexes is:

$$v_{ij} = (\max_j x_j - x_{ij})/(\max_j x_j - \min_j x_j) \tag{3}$$

Step 3) Constructing the weighted decision matrix

The dimensionless matrix is multiplied by the weight of each index (in general, the weight is originated from the Analytic Hierarchy Process (AHP) method [32], this method is subjective and may affect the evaluation results.) and Obtain weighted decision matrix $R = (r_{ij})_{m\times n}$.

$$r_{ij} = w_i * v_{ij} \quad (i = 1, 2.\ldots.m; j = 1, 2\ldots n) \tag{4}$$

Step 4) Computation of ideal solutions and negative ideal solutions

The ideal solution is:

$$S^+ = \max_{1\le i\le m} \{r_{ij}\} \quad (j = 1, 2\ldots n) \tag{5}$$

The negative ideal solution is:

$$S^- = \min_{1\le i\le m} \{r_{ij}\} \quad (j = 1, 2\ldots n) \tag{6}$$

Step 5) Calculating the distance

Distance from ideal solution:

$$Sd_i^+ = \sqrt{\sum_{j=1}^{n} \left(s_j^+ - r_{ij}\right)^2} \quad (i = 1, 2\ldots m; j = 1, 2\ldots n) \tag{7}$$

Distance from negative ideal solution:

$$Sd_i^- = \sqrt{\sum_{j=1}^{n} \left(s_j^- - r_{ij}\right)^2} \quad (i = 1, 2\ldots m; j = 1, 2\ldots n) \tag{8}$$

Step 6) Calculating the relative proximity and making decisions

Calculating relative proximity degree ζ_i formula is as follows:

$$\zeta_i = Sd_i^- / (Sd_i^+ + Sd_i^-) \tag{9}$$

Its value ranges from 0 to 1. The scheme with the biggest ζ_i is the best scheme.

B. TOPSIS METHOD BASED ON INFORMATION ENTROPY

Since the weight of the traditional TOPSIS method is determined by AHP method, the weight based on expert in AHP scores is a subjective method. Sometimes errors in subjective factors can lead to deviations or errors in the final decision result. Entropy method can reflect the orderliness of data information objectively. It determines the weight of the index by the judgment matrix, so as to eliminate the subjectivity of the weight of each factor as much as possible.

According to the definition of entropy, m schemes and n evaluation indexes, the entropy of evaluation indexes can be determined as follows:

$$H_j = \frac{1 + v_{ij}}{-ln\,(m)} * (\sum_{i=1}^{m} f_{ij} \ln\left(f_{ij}\right)) \quad (i = 1 \ldots m; j = 1 \ldots n) \tag{10}$$

v_{ij} is from Formula (2) or (3) and

$$f_{ij} = (1 + v_{ij}) / \sum_{i=1}^{m} 1 + v_{ij} \tag{11}$$

The entropy weight of each evaluation index is:

$$\omega_j = \frac{1 - H_J}{n - \sum_{j=1}^{n} H_j}, \sum_{j=1}^{n} \omega_j = 1 \tag{12}$$

C. PSO AND ITS IMPROVEMENT

Particle swarm optimization (PSO) is an optimization algorithm based on bird predation proposed by Kennedy in 1995 [33]. Suppose there is a piece of food in the area (optimal solution). Birds pass information to each other in the process of finding food, and cooperate to determine whether they can find the optimal solution. At the same time, the information of the optimal solution is transmitted to the whole bird population, and finally the optimal solution is obtained.

PSO particles have two properties, position X and velocity V. The velocity represents the direction of the particle and the position represents the current particle's solution. Each particle searches for the optimal solution in space, which is recorded as the current individual extreme value P_{best}, and uses the optimal individual extreme as the global optimal solution G_{best} for the entire particle swarm. Particles in the particle swarm update their velocities and positions according to P_{best} and G_{best}. The updated formulas for position and velocity are as follows:

$$\begin{aligned} V_{id}^{t+1} &= \omega V_{id}^{t} + C_1 * R\,(0, 1) * \left(P_{id} - X_{id}^{t}\right) \\ &\quad + C_2 * R\,(0, 1) * \left(P_{gd} - X_{id}^{t}\right) \end{aligned} \tag{13}$$

$$X_{id}^{t+1} = X_{id}^{t} + V_{id}^{t} \tag{14}$$

In the formula (13) and (14), d is the number of dimensions in the search space, i is the number of particles. ω is inertial weight, $R\,(0, 1)$ is a random number in between 0 and 1. The more the value ω, the more the global search ability and the weaker the local search ability, and vice versa. V_{id}^{t} is the velocity of i particle in the t th iteration of d-dimensional vector , X_{id}^{t} is the position of i particle in the t th iteration of d-dimensional vector. C_1C_2 is used as the accelerating factor to adjust the iteration step and usually takes [0,2]. P_{id} is the best individual position at present , P_{gd} is the global optimal position at present.

The farther C_1C_2 are from 2, the greater the impact of initial position on the iteration process is. According to the characteristics of the object, it is necessary to select the appropriate C_1C_2 values. When the complexity of the system is higher or the system is easier to fall into local optimum, it is necessary to select the smaller C_1C_2 value. For simple objects or systems, it is easy to select larger C_1C_2 value. According to the battery prediction condition in this paper, it is suggested that $C_1 = 1.85$ to make the variance smaller between the optimal position and the local optimal value in order to reduce the system oscillation. $C_2 = 2$ is selected to make the optimal position be closest to the global optimal value and to accelerate the optimization speed.

Other studies [34] showed that a larger inertial weight ω can avoid local minimum and a smaller inertial weight is helpful for convergence speed. In order to improve the global search ability, we give a larger value of the inertial weight in the initial stage of the search. Then, set the inertial weight to a smaller value to accelerate the convergence rate in the later stage of search.

Generally, linear decreasing inertia strategy is used to control weight.

$$\omega\,(t) = \omega_{begin} + \frac{\omega_{end} - \omega_{begin}}{t_{max}} * t \tag{15}$$

$\omega\,(t)$ is the change function, t is the number of iterations, ω_begin is the initial weight , ω_end is the final weight. After testing, select $\omega\_begin = 0.9$ and $\omega\_end = 0.4$.

Although the linear decreasing inertia strategy is simple, it sometimes converges too slowly. The improved method is to choose a larger ω value at the beginning of the iteration so that the particle can accelerate for a short time. Near the final stage of optimization, a smaller ω value is chosen to optimize accurately. Therefore, the linear decrease of ω changes as the following expressions:

$$\omega\,(t) = \left(\frac{t}{n}\right)^{m} * \omega_{begin} + \frac{\omega_{end} - \omega_{begin}}{t_{max}} * t \tag{16}$$

m is the decreasing index and n is the iterator threshold (usually about 1500).When the number of iterator t reaches n, set $\omega(t) = \omega\_begin$.

In summary, the process of the improved particle swarm optimization is as follows:

Step1) Determine the fitness function.

The minimum value of RMSE is chosen as the fitness function in this paper:

$$f\,(x) = min(\sqrt{\frac{1}{n} * \sum_{i=i}^{n} (x_i - y_i)^2}) \tag{17}$$

Step2) Initialize the velocity and position of the particle population and set the initial parameters of the algorithm.

Step3) Evaluation of particle fitness with (17).

Step4) For each particle, compare its current fitness with P_{id} and update P_{id}.

Step5) For each particle, compare its current fitness with P_{gd} and update P_{gd}.

Step6) Calculate and update the velocity and position of particles iteratively according to (11).

Step7) If the algorithm reaches the maximum number of iterations n or the optimal fitness is less than the given threshold, the algorithm stops and returns the result, otherwise, goes back to step three and continues iteration.

D. MOVING AVERAGE FILTER

Based on the statistical laws, the moving average filter (MAF) treats the continuous sampled data as a fixed-length N queue. After a new measurement, the first data of the above queue is removed and the remaining N-1 data is removed forward in sequence. The sampled data is inserted as the tail of the new queue. Then the arithmetic mean of the cohort is calculated and is treated as the measurement result [35]. Fig. 1. shows the implement structure diagram of a moving average filter system.

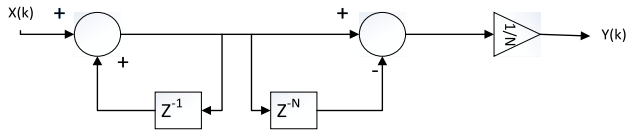

FIGURE 1. Structure diagram of a moving average filter system.

We can see that MAF has high computational efficiency. For a fixed-length window, it requires only one multiplication, one addition and one subtraction.

IV. THE PROPOSED PREDICTION SCHEME

The flow chart of the proposed prediction scheme is shown in Fig. 2. Firstly, a correlation test and a moving mean filter are used to eliminate the spike burr of data and to smooth the data., which is detailed in Part A in section V. Secondly the appropriate predictive parameters are selected by the TOPSIS method based on entropy weight, which is detailed in Part B in section V. Thirdly, the improved PSO algorithm is used to fit the parameters of the model and the RUL of the lithium-ion battery is predicted, which is detailed in Part C in section V. Finally, the comparative experimental analysis are done on parameters selection and RUL accuracy comparisons among several data-driven methods, which is detailed in Part D in section V.

V. TEST RESULTS ANALYSIS

A. BATTERY DATA DENOISING AND PARAMETERS CORRELATION TEST

The batteries data used in this paper is from NASA PcoE Research Center and with the same specifications and

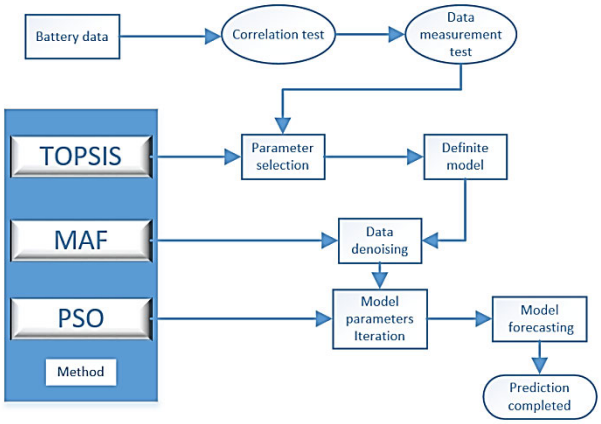

FIGURE 2. The flow chart of the proposed prediction scheme.

batches. These batteries are 18650 commercial lithium-ion batteries. The batteries are charged under 1.5A constant current (cc) mode at different room temperature until their voltage reaches 4.2V. Then the batteries continue to be charged under constant voltage (cv) mode until the charging current of the battery drops to 20mA. Finally, the batteries are discharged with 2A discharge current until its voltage drops to 2.7V. The impedance of the batteries is measured by electrochemical impedance spectroscopy (EIS) sweep from 0.1Hz to 5kHz. B5 and B6 battery are selected as the battery data set at room temperature, B40 battery is used for the low temperature battery dataset, B32 battery is used for the high temperature battery dataset. The change of SOH at different operating temperatures is shown in Fig. 3.

From the Fig. 3, we can see that the raw battery data has many spikes which are circled. We can see that data noise pollution is serious, so it will affect the accuracy of the prediction in the subsequent battery prediction stage.

Fig. 4 shows the effect of filtering by MAF filtering method.

From Fig. 4 we can see that MAF method can eliminate the spike of battery data. MAF filter is very simple and can effectively remove spikes and noise from battery data. So in the later work, the data used for prediction will be filtered by MAF, from Fig. 3 we can observe that the SOH declining trend of batteries at different temperatures is quite different. A battery used at room temperature has a gentler decay curve with fewer peaks and less fluctuation than a battery used at low and high temperatures. Under the high temperature working environment, the battery showed a huge fluctuation and a sharp decline trend, and it soon reached EOL. Therefore, temperature is the most important factor affecting the life of a lithium-ion battery. We choose Arrhenius model to study the relationship between SOH drop and temperature in lithium-ion batteries, because the Arrhenius model was usually used to represent the effect of temperature stress on product failure. The Arrhenius model formula is as follows:

$$Q_{loss} = A_0 * \exp\left(-\frac{Ea}{RT}\right) * Ah \tag{18}$$

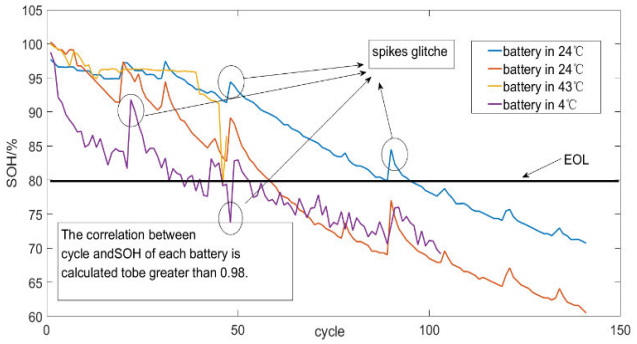

FIGURE 3. SOH and cycle charts of batteries at different temperatures.

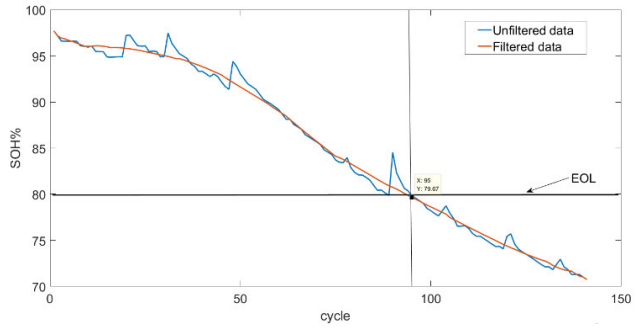

FIGURE 4. Battery data comparison before and after filtering.

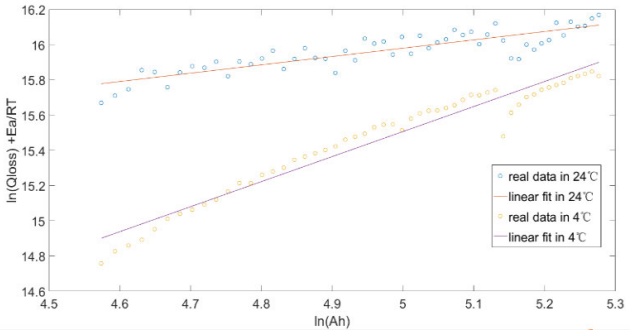

FIGURE 5. Temperature effect in 24°C and 4°C.

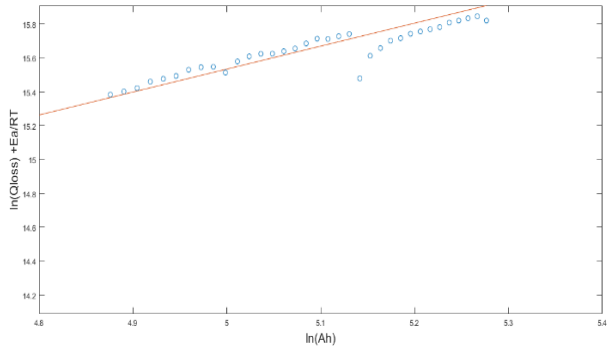

FIGURE 6. Temperature effect in 43°C.

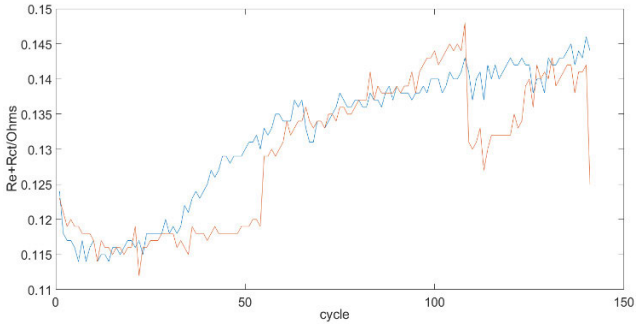

FIGURE 7. Parametric curve of Internal Resistance.

In formula (18) Q_{loss} is the percentage of battery loss, i.e. (1-SOH)%. A_0 is the pre-exponential factor; Ea is activation energy and it is 31500 J mol-1 by testing; R is Boltzmann constant, T is Kelvin;Ah = (*cycle number* ∗ *full battery capacity*). Select *Ah* instead of *cycle number* because the initial capacity of each battery is different. Take the natural logarithms on both sides of formula (18) and convert it to:

$$\mathrm{Ln}\,(Q_{loss}) + \mathrm{Ea/RT} = \mathrm{Ln}(A_0) + \mathrm{Ln}(\mathrm{Ah}) \qquad (19)$$

Batteries operating at room temperature (24°C) and at low temperature (4°C) were selected to fit the curve according to formula (19). The results are shown in Fig. 5:

High temperature (43 °C) batteries are fitted and displayed separately due to insufficient data. It is shown in Fig. 6:

From the linear relationships fitted in Fig. 5 and 6, the temperature effect does follow the Arrhenius model. The correlation coefficients of curve fitting are all above 0.95, corresponding to the thermal activation process.

Fig. 7 shows the internal resistance curve of lithium-ion batteries at room temperature of 24 °C.

From Fig. 7 we can observe that the internal resistance of batteries operating at room temperature (24 °C) increases with the rise of cycle. After calculation, the correlation coefficient between internal resistance and number of cycles also exceeds 0.9. Therefore, internal resistance can be used as an aging parameter to predict the RUL of batteries. However, similar to SOH degradation curve, due to environmental and operational factors, the internal resistance also has a large number of spikes and fluctuations. Therefore, we still need MAF filtering for internal resistance parameters. Fig. 8 shows the result.

It can be seen that the filtered curve is smoother without distortion. Therefore, it is more suitable for the prediction of lithium-ion batteries. In later experiments, data will be processed by MAF filters.

Fig. 9 shows the internal resistance curve of a battery operating at 43 and 4 degrees.

From Fig. 9 we can observe that the variation regularity of internal resistance at high and low temperatures is not strong, and the correlation coefficient with cycle is less than 0.5, the fluctuation is huge. Therefore, the following section will prove that internal resistance is not suitable for battery prediction at high temperature and low temperatures.

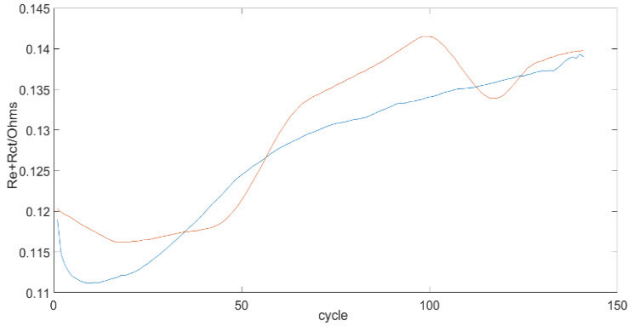

FIGURE 8. Parametric Curves of Internal Resistance after Filtering.

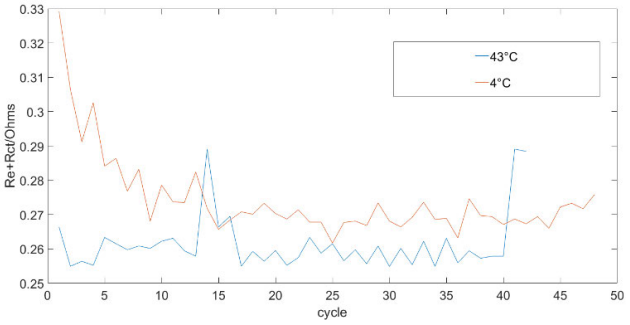

FIGURE 9. Internal Resistance curve at high and low temperatures.

Fig. 10 shows the open-circuit voltage curve of lithium-ion batteries at room temperature of 24 °C.

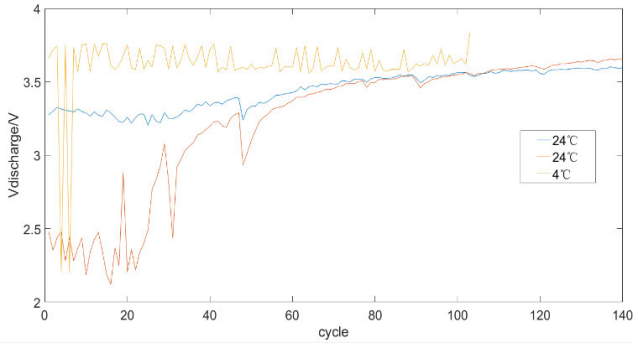

FIGURE 10. Open-circuit voltage curves at different temperatures.

As the open-circuit voltage data is insufficient in a working environment of 43 degrees, it is not shown in the figure because too few data is meaningless for the subsequent prediction work. We can observe that the open-circuit voltage of the battery shows a good trend at room temperature, and the fluctuation is also small in Fig. 8. At low temperature, the voltage fluctuates sharply at the beginning and there is no obvious trend of increase or decrease about the curve. Therefore, the selection of open-circuit voltage is uncertain in TOPSIS parameter selection method at low and high temperatures.

The open-circuit voltage curve after filtering is shown at Fig. 11.

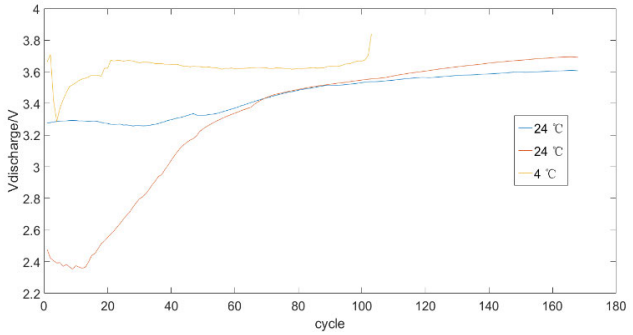

FIGURE 11. Open-circuit voltage curves at different temperatures after filter.

B. PARAMETERS SELECT OF BATTERY DEGRADATION MODEL

From the figures and data in the previous section, we can see that there is insufficient data for some parameters at different temperatures, for example, open-circuit voltage of batteries at high temperature and low temperatures in Fig. 10. Sometimes the data fluctuates too much which might affect battery prediction as shown in Fig. 9. However, most references do not change the predictive parameters according to different working conditions and the changes of parameter data such as references [13], [17]–[19]. And this will have a certain impact on the accuracy of battery prediction. Therefore, we need to select different degradation parameters using TOPSIS method based on information entropy for battery prediction under different conditions.

The flowchart of select parameters by TOPSIS method is shown in Fig. 12.

Through the analysis of section II and section V.A of this article, temperature (T), internal resistance (Re+Rct), open-circuit voltage (OCV) and cycle number (CycleNum) are selected as the set of parameters to be selected by TOPSIS method. For the index we select: 1. The amount of data. The reason is that the amount of data is the basis of battery prediction. If the amount of data is missing too much, it will inevitably affect the accuracy of battery prediction and may cause errors; 2. Correlation coefficient between parameter data and SOH. The correlation coefficient is a statistical index used to reflect the degree of close correlation between variables, reflecting the relationship between the two variables. If there is no relationship or weak relationship between the predicted parameters and the predicted values, it is meaningless to use this parameter to predict, which will directly lead to the distortion and reduce the accuracy of the predicted results; 3. The fluctuation degree of the battery data (we choose variance to describe the fluctuation of data) Because there is a direct functional relationship between the predicted parameters and the predicted results, if the fluctuation of the predicted parameters is too large, it will indirectly affect the predicted results and make the fluctuation of the predicted results larger. Therefore, the prediction parameters are also the necessary parameters optimization index; 4. A subjective index which represents how much each parameter correlates

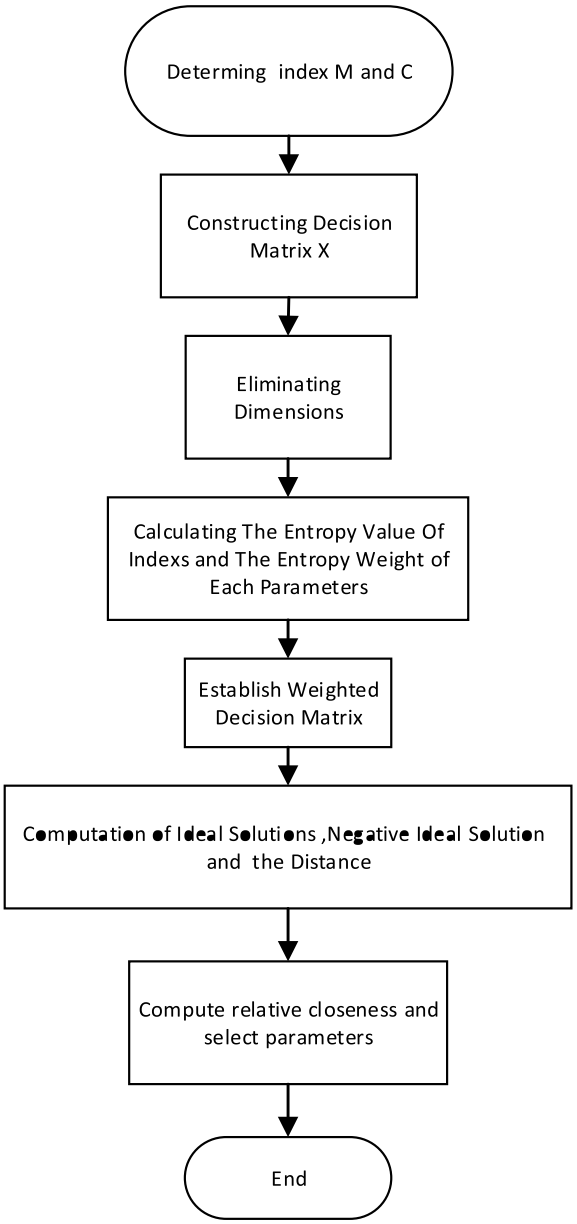

FIGURE 12. TOPSIS based on information entropy Flow Chart.

with battery life degradation. The 4th index is the subjective result obtained by comprehensively analyzing the battery prediction parameters used by predecessors, the physical and chemical properties of batteries, and the physical and chemical relationship of battery degradation.

Based on the above conclusions, we can define Decision matrix, as shown in Table 1:

Table 2 shows the decision matrix at room temperature. Each value in the matrix ranges from 0 to 10 where the best quality parameter is specified to 10 under each index. Because the values of each index could not be exactly 10, for example, the maximum correlation coefficient is 1 and the minimum is 0, so the final results should be changed to the range of 0-10 proportionally.

TABLE 1. The form of decision.

/	Data volume	correlation coefficient	Fluctuation degree	Subjective
CycleNum	X11	X12	X13	X14
Temperature	X21	X22	X23	X24
Vdischarge	X31	X32	X33	X34
Re+Rct	X41	X42	X43	X44

TABLE 2. Decision matrix.

/	Data volume	correlation coefficient	Fluctuation degree	Subjective
CycleNum	10	9.8	10	10
Temperature	10	9.5	10	9
Vdischarge	10	9.6	7	8
Re+Rct	10	7	3	8

The normalized matrix using (2), (3) is shown in Table 3.

The entropy weight of each index can be calculated by formula (11), (12), (13) as follows: Data quantity: 0.012, Correlation coefficient: 0.277, Fluctuation degree: 0.0289, Subjective: 0.421.

By multiplying the corresponding weight value for each item in the matrix of Table 3 We can get the weighted decision matrix shows in Table 4.

TABLE 3. Normalized matrix.

/	Data volume	correlation coefficient	Fluctuation degree	Subjective
CycleNum	1	1	1	1
Temperature	1	0.89	1	0.5
Vdischarge	1	0.92	0.57	0
Re+Rct	1	0	0	0

TABLE 4. Wrighted decision matrix.

/	Data volume	correlation coefficient	Fluctuation degree	Subjective
CycleNum	0.0030	0.0812	0.0906	0.1276
Temperature	0.0030	0.0767	0.0906	0.1145
Vdischarge	0.0030	0.0778	0.0709	0.0766
Re+Rct	0.0030	0.0404	0.0453	0.0766

The positive ideal solution vector is:
(0.0030 0.0812 0.0906 0.1276)
The negative ideal solution vector is:
(0.0030 0.0404 0.0453 0.0766)
Through formula (7), (8), (9), the relative proximity of each parameter is:

$\zeta_{cyc} = 1.000$, $\zeta_{temp} = 0.833$, $\zeta_{Vdis} = 0.452$, $\zeta_R = 0$

Generally speaking, the difference of relative proximity is more than one order of magnitude, which indicates that the disparity between the two schemes is too large, and the parameters with small relative proximity should be discarded. So we choose CycleNum, temperature, Vdischarge, as the predictive parameter of batteries at room temperature.

Through the steps shown above, the Decision matrix of the battery at low temperature is shown in Table 5.

TABLE 5. Decision matrix of battert at low temperature.

/	Data volume	correlation coefficient	Fluctuation degree	Subjective
CycleNum	10	9.2	10	10
Temperature	10	8.7	10	9
Vdischarge	10	1.3	3.4	8
Re+Rct	10	0	3.2	8

The relative proximity of each parameter is:

$\zeta_{cyc} = 1.000$, $\zeta_{temp} = 0.748$, $\zeta_{Vdis} = 0.052$, $\zeta_R = 0$

So we choose CycleNum and temperature as the predictive parameter of batteries at low temperature.

The Decision matrix of the battery at high temperature is shown in Table 6.

TABLE 6. Decision matrix of battert at high temperature.

/	Data volume	correlation coefficient	Fluctuation degree	Subjective
CycleNum	10	9.2	10	10
Temperature	10	4.3	10	9
Vdischarge	6	0	0	8
Re+Rct	6	0	0	8

Because the amount of data of batteries in high temperature working environment is too small, it is meaningless to judge the correlation coefficient and fluctuation degree of batteries. Therefore, the correlation coefficient and fluctuation degree of open-circuit voltage and internal resistance parameters are all 0.

The relative proximity of each parameter is:

$\zeta_{cyc} = 1.000$, $\zeta_{temp} = 0.092$, $\zeta_{Vdis} = 0$, $\zeta_R = 0$

So only CycleNum is selected as the predictive parameter for RUL prediction at high temperature.

C. CURVE FITTING RESULTS OF IMPROVED PARTICLE SWARM OPTIMIZATION

According to Section III part C, we can get the flow chart of the improved particle filter algorithm, which is shown as in Fig. 13.

Generally, the parameters used to judge the curve fitting results are root of mean square error (RMSE), residual sum of squares (SSE), correlation coefficient (R), determination coefficient (R-sqare). RMSE is the fitting standard deviation of regression system. Generally, the RMSE value is smaller, the result is better. SSE is sum variance. The statistical parameter calculates the square of the error between the fitting data and the corresponding points of the original data. The closer the SSE value is to 0, the better fitting effect. The Correlation Coefficient(R) represents the degree of correlation between fitting curve and original curve. The closer the R value is to 1, the greater correlation. R-sqare is the change of data to represent the quality of a fitting. The value range is between 0 and 1. The closer the R-sqare value

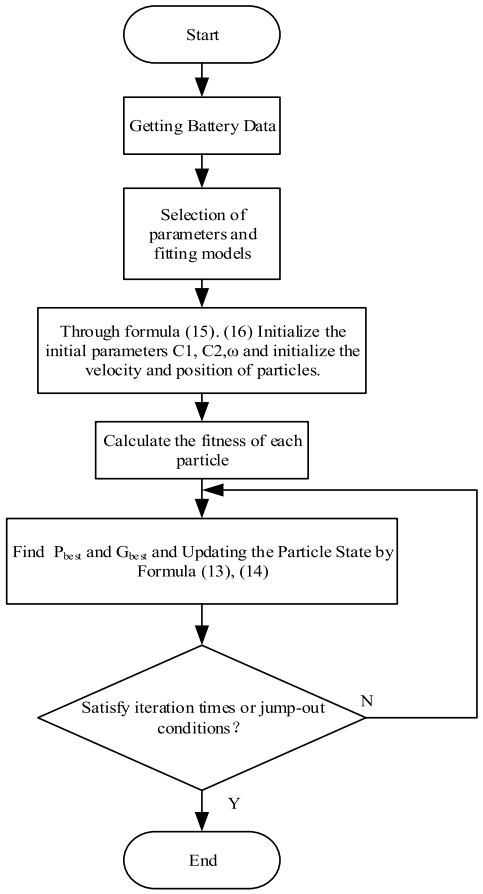

FIGURE 13. Flow chart of improved particle filter algorithm.

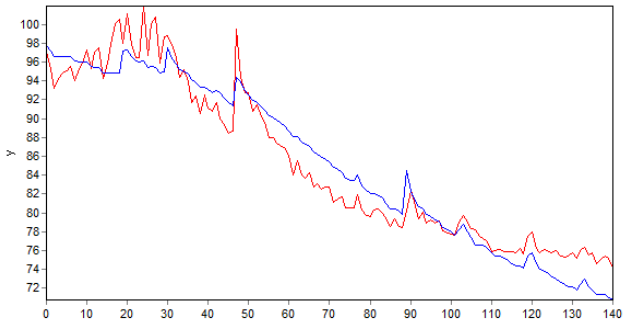

FIGURE 14. The original particle Swarm Optimization.

is to 1, the greater the correlation. We use particle swarm optimization, improved particle swarm optimization, genetic algorithm and Particle filtering algorithm to fit the battery data under standard operating conditions. The fitting results are shown in Fig.14-Fig.17. The blue curve represents the original data, and the red curve represents the fitted data. The abscissa in the figure means the number of battery charge and discharge cycles, and the ordinate means the battery's SOH. The fitting equation is as follows:

$$y = a1 * cycle^2 + a2Vdischarge + a3exp(-Ea/RT) + a4 \quad (20)$$

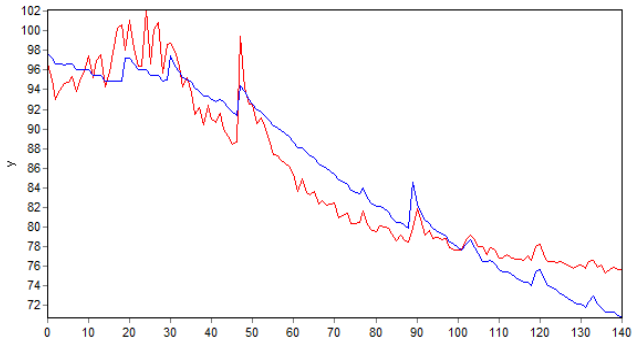

FIGURE 15. The genetic Algorithm.

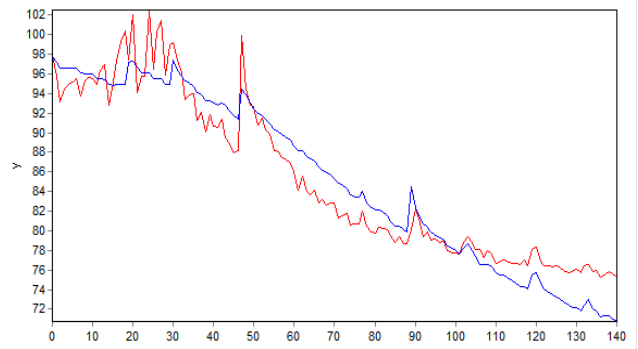

FIGURE 16. The particle filtering algorithm.

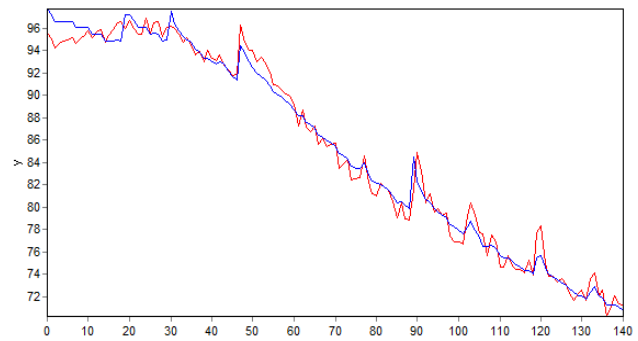

FIGURE 17. The improved particle swarm optimization.

Among them, a1, a2, a3 and a4 are fitting parameters, cycle is the number of charge and discharge cycles of batteries, Vdischarge is open-circuit voltage *Ea* is activation energy, *R* is Boltzmann constant and *T* is the absolute temperature.

It can be seen from Fig. 14-17 that the improved particle swarm algorithm has better convergence and accuracy than the original particle swarm algorithm and other related algorithms in fitting the curve.

The four parameters RMSE, SSE, R, R-square of each fitting curve are shown in the Table 7.

From the table 7 above, we can see that compared with the original PSO, Particle filtering(PF) algorithm and other fitting algorithms [2], [3], [18], the improved PSO has smaller fitting error, higher fitting degree and better accuracy. So we choose the improved particle swarm optimization algorithm to fit the battery life prediction parameters.

TABLE 7. Parameters of Fitting Results of algorithm.

Fitting algorithm	RMSE	SSE	R	R-square
Particle swarm optimization	2.4137	821.5260	0.9616	0.9248
genetic algorithm	2.6761	1009.795	0.9527	0.9076
particle filtering	2.5877	944.2296	0.9561	0.9141
Improved particle swarm optimization	0.9837	136.4560	0.9937	0.9875

D. COMPARATIVE EXPERIMENTAL ANALYSIS

Based on the TOPSIS method and the conclusions drawn from Figure 24-26, we choose CycleNum, temperature, Vdischarge as the predictive parameters of batteries at room temperature under standard operating conditions. And use formula (20) as the model for battery prediction.

In order to verify the battery prediction method proposed in this paper, we provide four schemes for comparison experiments.

In the first scheme, we select the battery data without MAF filtering to predict the battery RUL. We use battery data from the first 40 cycles to train parameters. After training, we use the model to predict the battery RUL and compare it with the original battery data. Formula (20) is selected as the battery RUL prediction model. The predicted results are shown in the Fig. 18.

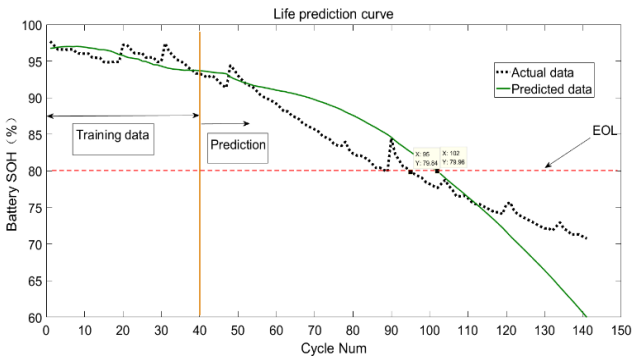

FIGURE 18. Prediction of battery RUL without filtering.

In the second scheme, we only select the cycle number as the parameter of battery RUL prediction. After MAF filtering, we use the battery data from the first 40 cycles to train the parameters. After training, we use this model to predict the battery RUL and compare it with the original battery data. The fitting equation is as follows:

$$y = a1cycle^2 + a2cycle + a3 \tag{21}$$

The predicted results are shown in the Fig. 19.

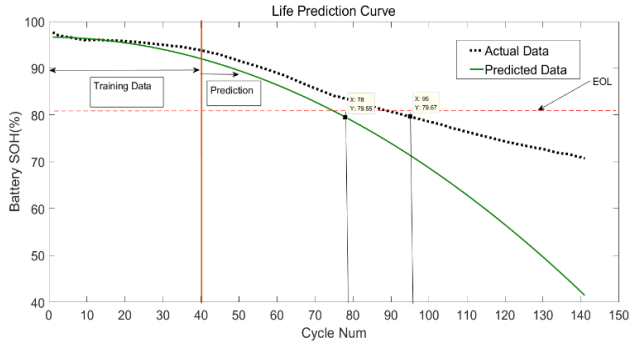

FIGURE 19. Battery RUL prediction data after data filtering with the parameter which with only one parameter (CycleNum).

In the third scheme we select the cycle number, internal resistance of battery Re+Rct, Vdischarge as the parameter of battery RUL prediction. After MAF filtering, we use the battery data from the first 40 cycles to train the parameters. After training, we use this model to predict the battery RUL and compare it with the original battery data, the fitting equation is as follows:

$$y = a1cycle^2 + a2Vdischarge + a3\,(Re + Rct) + a4 \quad (22)$$

The predicted results are shown in the Fig. 20.

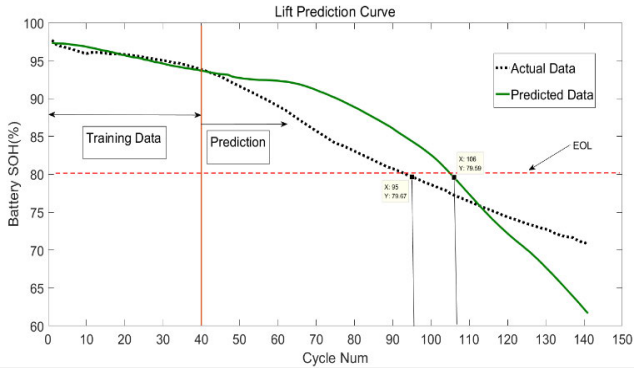

FIGURE 20. Battery RUL prediction data after data filtering with the parameter which with the parameter which are not be selected by TOPSIS method.

In the fourth scheme, we select the cycle number, temperature and Vdischarge as the parameter of battery RUL prediction, which are selected by the TOPSIS method in Chapter V, After MAF filtering, we use first 40 cycles of the battery data to train the parameters. After training, we use this model to predict the battery RUL and compare it with the original battery data. The fitting equation we use is Formula (20).

The predicted results are shown in the Fig. 21.

Table 8 shows the comparison results of the four schemes.

From Fig.18-21 and table 8 we can see that: (1) The effect of single parameter prediction is average, and the prediction curve has a large deviation. (2) The predicted results of raw data without MAF filter are quite different from the actual results. (3) The parameters obtained by the non-TOPSIS method have a great influence on the predictions, making the predicted results inaccurate. (4) After MAF filtering and TOPSIS method parameter optimization, the predicted results using PSO algorithm is quite accurate and has high accuracy.

TABLE 8. Comparison of four schemes.

Scheme	1	2	3	4
Prediction parameters	cycle,Vdischarge,temperature	Cycles	Cycles,Vdischarge,Re+Rct	cycles,Vdischarge,temperature
Methods used	PSO,TOPSIS	PSO	PSO,MAF	PSO,MAF, TOPSIS
Prediction results	7 Cycle late	17Cycle earlier	11 Cycle late	accurate
Training data points	40	40	40	40

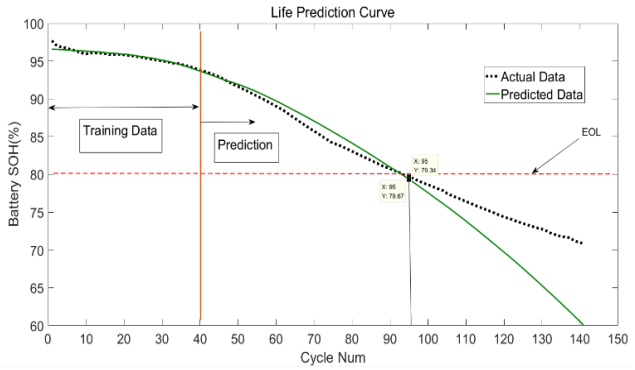

FIGURE 21. Battery RUL prediction data after data filtering with the parameter which are selected by TOPSIS method.

Different training data points were taken to train the model, and the first 20, 25, 30, 50 capacity measurement data points were taken to the experiment. The predictions at 20, 25, 30, 50 and 100 cycles are shown in Fig. 22, Fig. 23, Fig. 24 and Fig. 25.

The predictions of different data points are shown in Table 9.

TABLE 9. Prediction results of different training points.

Data points	20	25	30	40	50
Prediction results	30 Cycle late	10 Cycle late	accurate	accurate	accurate

From Table 9, we can see that the predicted results obtained by different training data points are different. As the number of data points increases, the accuracy of the model improves and eventually reaches convergence.

Finally we experiment with different data sets. Fig.26 shows the battery prediction results of the University of Maryland lithium-ion battery cycle life experiment, the battery number is A12.

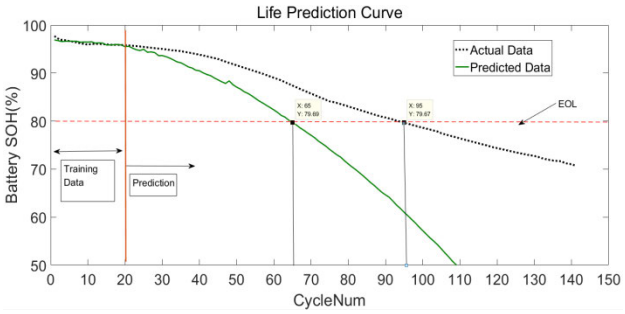

FIGURE 22. Predict results of 20 data points.

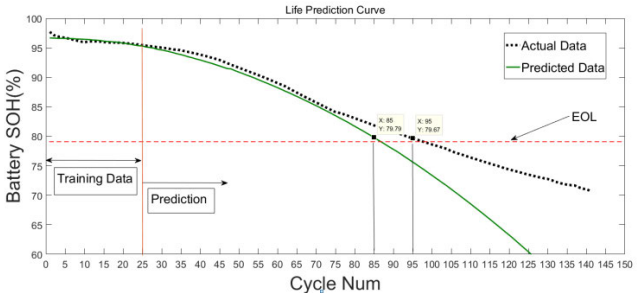

FIGURE 23. Predict results of 25 data points.

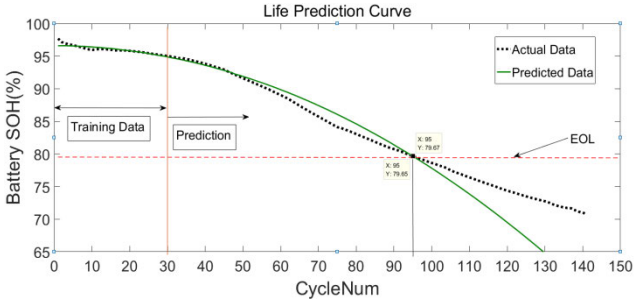

FIGURE 24. Predict results of 30 data points.

Because the battery experiment data is insufficient, CycleNum can only be selected as the battery model parameter.

It can be seen from Fig.26 that we use 70 training data points to train the model and the predicted result is 6 cycles earlier than the real result, The prediction result is accurate but have a certain deviation, the reason may be that the lack of other battery data makes the battery model inaccurate.

E. COMPARISON WITH OTHER PREDICTION METHODS AND TEST UNDER HIGH AND LOW TEMPERATURE

To illustrate the advantage of our proposed frameworks, we have done some comparison experiments among some frequently-used data-driven RUL prediction algorithms such as particle filter (PF), support vector regression (SVR), neural network (NN), and our method. The comparison results are shown in Table 10.

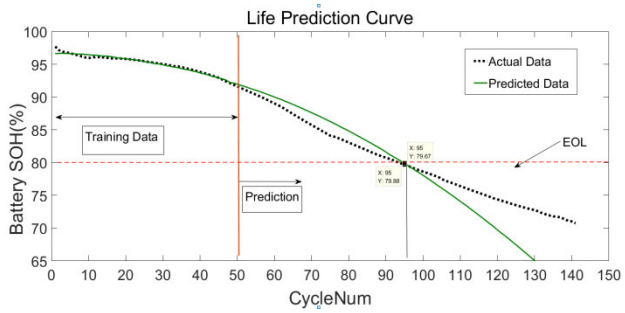

FIGURE 25. Predict results of 50 data points.

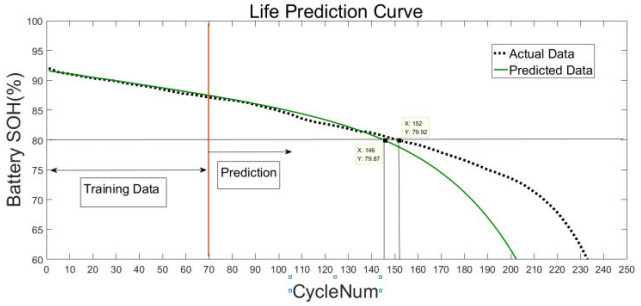

FIGURE 26. University of Maryland battery data prediction results.

TABLE 10. Comparison with other methods.

Corresponding reference	2	3	7	16	This Paper
Prediction method	PF and SVR	Improved PF	local information fusion with SVR	LSTM Neural Networks	PSO,MAF,TOPSIS
Prediction parameters	Re+Rct, cycles	cycles	cycles	cycles	cycles,V discarge ,temperature
Training data points	50	35	80	100	40
Prediction results	11Cycle late	10Cycle earlier	5Cycle earlier	2Cycle earlier	accurate

From table 10 We can see that our method has higher prediction accuracy and use less training data than other data-driven algorithms. Under the condition of 40 training data, the prediction results are almost accurate. Neural network algorithms need more training data to get higher accuracy, for example, the LSTM method [16] needs 100 training data points to get more accurate prediction results. The PF and SVR methods [2], [3], [7] got lower prediction accuracy through 50 training data points. Therefore, the method described in this paper is more suitable for the RUL prediction of lithium-ion batteries.

Furthermore, most of other methods cannot get the prediction results of the battery at high and low temperature.

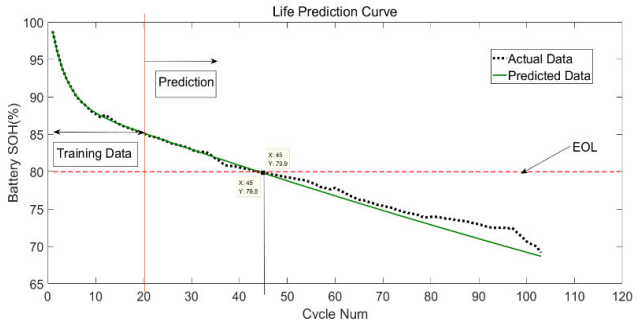

FIGURE 27. Predict results of battery at high temperature.

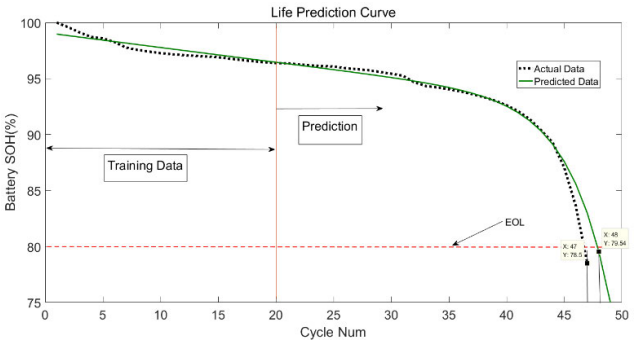

FIGURE 28. Predict results of battery at low temperature.

In order to verify the robustness of our method, the RUL value of the battery under high and low temperature conditions is predicted using our method. The results are shown in Fig.27-28.

As shown in Figures 27 and 28, the RUL prediction results of the methods described in this paper are still accurate under high and low temperature conditions. Therefore, the proposed method not only has higher accuracy and less data training, but also guarantees the predicted results under high and low temperature conditions.

VI. CONCLUSION

A RUL estimation method for lithium-ion batteries based on improved particle swarm algorithm (PSO) and TOPSIS is proposed in this paper. The work focuses on the following aspects: (1) Optimizing the parameters involved in battery RUL prediction by using the TOPSIS method based on entropy weight, and selecting appropriate parameters for prediction; (2) Using MAF filter to perform battery raw data filter to get a smooth battery life degradation curve. (3) Using the improved particle swarm algorithm to make RUL prediction more accurate.

By comparing many experimental cases including under high and low temperature conditions, our method can achieve more accurate battery RUL prediction and acceptable performance threshold under different battery conditions. Compared with the other data-driven RUL prediction algorithms, our method has the following advantages: (1) The prediction accuracy of our algorithm is higher than that of other prediction algorithms; (2) Our method requires a smaller amount of sampled data; (3) Our method are also accurate and robust under high and low temperature conditions.

ACKNOWLEDGMENT

The authors would like to thank NASA Ames Prognostics Center of Excellence (PCoE) and University of Maryland (UMD) for their lithium-ion battery experimental data.

REFERENCES

[1] L. Datong *et al.*, "Lithium-ion battery health assessment and life prediction review," *J. Instrum. Instrum.*, vol. 36, no. 1, pp. 1–16, Jan. 2015, doi: 10.3969/j.issn.1672-6413.2015.01.004.

[2] J. Wei, G. Dong, and Z. Chen, "Remaining useful life prediction and state of health diagnosis for lithium-ion batteries using particle filter and support vector regression," *IEEE Trans. Ind. Electron.*, vol. 65, no. 7, pp. 5634–5643, Jul. 2018, doi: 10.1109/tie.2017.2782224.

[3] Z. Jin, W. Ying, H. Yusheng, Z. Wenda, and Z. Feng, "An improved algorithm for predicting the remaining life of lithium-ion batteries," *Appl. Electron. Technique*, vol. 41, no. 8, pp. 110–112,116, Jan. 2015, doi: 10.16157/j.issn.0258-7998.2015.08.031.

[4] T. Weichi, *Spacecraft Systems Engineering*. Hefei, China: Anhui Province, 2014 pp. 100–115.

[5] N. Williard, W. He, C. Hendricks, and M. Pecht, "Lessons learned from the 787 dreamliner issue on lithium-ion battery reliability," *Energies*, vol. 6, no. 9, pp. 4682–4695, Sep. 2013, doi: 10.3390/en6094682.

[6] A. E. Mejdoubi, A. Oukaour, H. Chaoui, H. Gualous, J. Sabor, and Y. Slamani, "State-of-charge and state-of-health lithium-ion batteries' diagnosis according to surface temperature variation," *IEEE Trans. Ind. Electron.*, vol. 63, no. 4, pp. 2391–2402, Apr. 2016.

[7] J. Chen, J. Hou, X. Wang, H. Shao, G. Song, and Y. Xue, "Prediction for state of health of lithium-ion batteries by local information fusion with ensemble support vector regression," *J. Nanjing Univ. Sci. Technol.*, vol. 42, pp. 48–55, Feb. 2018, doi: 10.14177/j.cnki.32-1397n.2018.42.01.007.

[8] H. Chaoui, N. Golbon, I. Hmouz, R. Souissi, and S. Tahar, "Lyapunov-based adaptive state of charge and state of health estimation for lithium-ion batteries," *IEEE Trans. Ind. Electron.*, vol. 62, no. 3, pp. 1610–1618, Mar. 2015, doi: 10.1109/TIE.2014.2341576.

[9] Y. Zhang, R. Xiong, H. He, and M. G. Pecht, "Long short-term memory recurrent neural network for remaining useful life prediction of lithium-ion batteries," *IEEE Trans. Veh. Technol.*, vol. 67, no. 7, pp. 5695–5705, Jul. 2018.

[10] F. Pagnanelli, E. Moscardini, P. Altimari, T. Abo Atia, and L. Toro, "Cobalt products from real waste fractions of end of life lithium ion batteries," *Waste Manage.*, vol. 51, pp. 214–221, May 2016, doi: 10.1016/j.wasman.2015.11.003.

[11] M. Dubarry and B. Y. Liaw, "Identify capacity fading mechanism in a commercial LiFePO4 cell," *J. Power Sources*, vol. 194, no. 1, pp. 541–549, Oct. 2009, doi: 10.1016/j.jpowsour.2009.05.036.

[12] K. Liu, Y. Li, X. Hu, M. Lucu, and W. D. Widanage, "Gaussian process regression with automatic relevance determination kernel for calendar aging prediction of lithium-ion batteries," *IEEE Trans. Ind. Informat.*, vol. 16, no. 6, pp. 3767–3777, Jun. 2020, doi: 10.1109/TII.2019.2941747.

[13] K. Liu, Y. Shang, Q. Ouyang, and W. D. Widanage, "A data-driven approach with uncertainty quantification for predicting future capacities and remaining useful life of lithium-ion battery," *IEEE Trans. Ind. Electron.*, early access, Mar. 18, 2020, doi: 10.1109/TIE.2020.2973876.

[14] K. Liu, C. Zou, K. Li, and T. Wik, "Charging pattern optimization for lithium-ion batteries with an electrothermal-aging model," *IEEE Trans. Ind. Informat.*, vol. 14, no. 12, pp. 5463–5474, Dec. 2018, doi: 10.1109/TII.2018.2866493.

[15] O. Erdinc, B. Vural, and M. Uzunoglu, "A dynamic lithium-ion battery model considering the effects of temperature and capacity fading," in *Proc. Int. Conf. Clean Electr. Power*, Capri, Italy, Jun. 2009, pp. 383–386.

[16] B. Long, X. Li, X. Gao, and Z. Liu, "Prognostics comparison of lithium-ion battery based on the shallow and deep neural networks model," *Energies*, vol. 12, no. 17, p. 3271, Aug. 2019.

[17] D. Wang, F. Yang, K.-L. Tsui, Q. Zhou, and S. J. Bae, "Remaining useful life prediction of lithium-ion batteries based on spherical cubature particle filter," *IEEE Trans. Instrum. Meas.*, vol. 65, no. 6, pp. 1282–1291, Jun. 2016, doi: 10.1109/TIM.2016.2534258.

[18] W. Xian, B. Long, M. Li, and H. Wang, "Prognostics of lithium-ion batteries based on the verhulst model, particle swarm optimization and particle filter," *IEEE Trans. Instrum. Meas.*, vol. 63, no. 1, pp. 2–17, Jan. 2014, doi: 10.1109/TIM.2013.2276473.
[19] Y. Zhang, Y. Zhang, Z. Liu, D. Guan, F. Wang, V. Meyers, C. Yuan, A. Neuber, and H.-C. Zhang, "Laser ablation on lithium-ion battery electrode solid electrolyte interface removal," *J. Laser Appl.*, vol. 29, no. 4, Nov. 2017, Art. no. 042002.
[20] R. C. Xu, X. L. Wang, S. Z. Zhang, Y. Xia, X. H. Xia, J. B. Wu, and J. P. Tu, "Rational coating of $Li_7P_3S_{11}$ solid electrolyte on MoS_2 electrode for all-solid-state lithium ion batteries," *J. Power Sources*, vol. 374, pp. 107–112, Jan. 2018, doi: 10.1016/j.jpowsour.2017.10.093.
[21] F. Dinkelacker, P. Marzak, J. Yun, Y. Liang, and A. S. Bandarenka, "Multistage mechanism of lithium intercalation into graphite anodes in the presence of the solid electrolyte interface," *ACS Appl. Mater. Interface*, vol. 10, no. 16, pp. 14063–14069, Mar. 2018, doi: 10.1021/acsami.7b18738.
[22] M. Xu, L. Xing, and W. Li, "Interphases between electrolytes and anodes in Li-ion battery," in *Electrolytes for Lithium and Lithium-Ion Batteries*. Ma. 2014, pp. 227–282, doi: 10.1007/978-1-4939-0302-3_5.
[23] K. Smith, M. Earleywine, E. Wood, J. Neubauer, and A. Pesaran, "Comparison of plug-in hybrid electric vehicle battery life across geographies and drive cycles," SAE Tech. Papers, Apr. 2012, doi: 10.4271/2012-01-0666.
[24] Y. Zhang, C.-Y. Wang, and X. Tang, "Cycling degradation of an automotive $LiFePO_4$ lithium-ion battery," *J. Power Sources*, vol. 196, no. 3, pp. 1513–1520, Feb. 2011, doi: 10.1016/j.jpowsour.2010.08.070.
[25] H. Ku, Y. Jung, M. Jo, S. Park, S. Kim, D. Yang, K. Rhee, E.-M. An, J. Sohn, and K. Kwon, "Recycling of spent lithium-ion battery cathode materials by ammoniacal leaching," *J. Hazardous Mater.*, vol. 313, pp. 138–146, Aug. 2016, doi: 10.1016/j.jhazmat.2016.03.062.
[26] J. Jaguemont, L. Boulon, and Y. Dube, "Characterization and modeling of a hybrid-electric-vehicle lithium-ion battery pack at low temperatures," *IEEE Trans. Veh. Technol.*, vol. 65, no. 1, pp. 1–14, Jan. 2016, doi: 10.1109/TVT.2015.2391053.
[27] D.-I. Stroe, M. Swierczynski, S. K. Kar, and R. Teodorescu, "Degradation behavior of lithium-ion batteries during calendar ageing—The case of the internal resistance increase," *IEEE Trans. Ind. Appl.*, vol. 54, no. 1, pp. 517–525, Jan. 2018, doi: 10.1109/TIA.2017.2756026.
[28] J. Vetter, P. Novák, M. R. Wagner, C. Veit, K.-C. Möller, J. O. Besenhard, M. Winter, M. Wohlfahrt-Mehrens, C. Vogler, and A. Hammouche, "Ageing mechanisms in lithium-ion batteries," *J. Power Sources*, vol. 147, nos. 1–2, pp. 269–281, Sep. 2005, doi: 10.1016/j.jpowsour.2005.01.006.
[29] H.-F. Yuan and L.-R. Dung, "Offline State-of-Health estimation for high-power lithium-ion batteries using three-point impedance extraction method," *IEEE Trans. Veh. Technol.*, vol. 66, no. 3, pp. 2019–2032, Mar. 2017, doi: 10.1109/TVT.2016.2572163.
[30] A. P. Schmidt, M. Bitzer, Á. W. Imre, and L. Guzzella, "Model-based distinction and quantification of capacity loss and rate capability fade in Li-ion batteries," *J. Power Sources*, vol. 195, no. 22, pp. 7634–7638, Nov. 2010, doi: 10.1016/j.jpowsour.2010.06.011.
[31] D. L. Olson, "Comparison of weights in TOPSIS models," *Math. Comput. Model.*, vol. 40, nos. 7–8, pp. 721–727, Oct. 2004, doi: 10.1016/j.mcm.2004.10.003.
[32] J. Kennedy and R. Eberhart, "Particle swarm optimization," in *Proc. IEEE ICNN*, vol. 4, Nov./Dec. 1995, pp. 1942–1948, doi: 10.1109/ICNN.1995.488968.
[33] R. C. Eberhart and Y. Shi, "Comparing inertia weights and constriction factors in particle swarm optimization," in *Proc. Congr. Evol. Comput. (CEC)*, La Jolla, CA, USA, vol. 1, 2000, pp. 84–88.
[34] A. Jadoon, "Moving average filter," U.S. Patent 6 304 133 B1, Oct 16, 2001.

BING LONG (Member, IEEE) received the M.S. degree from Harbin Engineering University, Harbin, China, in 2002, and the Ph.D. degree from the Harbin Institute of Technology, Harbin, in 2005. He is currently a Full Professor with the University of Electronic Science and Technology of China, Chengdu, China. He served as a General Secretary and a Publication Chair in IEEE ICTD, in 2009. He has published more than 100 scholarly articles, and authorized over ten patent declarations in China. His current research interests include failure analysis, automatic testing, diagnostics, prognostics and health management, and testability design and analysis for lithium-ion batteries, circuits and systems.

XIAOYU GAO received the B.S. degree in automation engineering from the University of Electronic Science and Technology of China, in 2013, where he is currently pursuing the M.S. degree in instrumentation engineering. His research interests include lithium-ion battery health management systems and predict the remaining useful life of lithium-ion battery.

Mr. Gao's awards and honors include the Academic second class scholarship, academic third class scholarship while studying for M.S. degree.

PENGCHENG LI received the B.S. degree in automation from Southwest Jiaotong University, in 2012. He is currently pursuing the M.S. degree in instrumentation engineering with the University of Electronic Science and Technology of China.

His research interests include prognostic and health management of hydrogen fuel cell. His awards and honors include the academic second class scholarship while studying for M.S. degree.

ZHEN LIU received the B.S. and M.S. degrees in electrical engineering and the Ph.D. degree in detection technology and automatic equipment from Northwestern Polytechnical University (NPU), Xi'an, China, in 1999, 2002, and 2007, respectively.

Since 2007, he has been working with the University of Electronic Science and Technology of China (UESTC), Chengdu, China, where he is currently a Professor with the Department of Instrument Science and Technology, School of Automation Engineering. From December 2013 to January 2015, he was a Visiting Scholar with the Department of Statistics and Applied Probability, University of California—Santa Barbara, CA, USA. He is currently the Research Director of the PHM (Prognostics and Health Management) Laboratory, Electronic Testing Technology and Instruments Engineering Research Center of the Ministry of Education of China. His research interests include testability analysis, fault diagnosis, fault prediction, and lifetime estimate technology based on the machine learning for electronic systems.